THE JOURNAL OF PHYSICAL CHEMISTRY B

Article

pubs.acs.org/JPCB

Effect of Organic Solvents on Li^+ Ion Solvation and Transport in Ionic Liquid Electrolytes: A Molecular Dynamics Simulation Study

Zhe Li,[†] Oleg Borodin,[‡] Grant D. Smith,[§] and Dmitry Bedrov*[,†,§]

[†]Department of Materials Science & Engineering, University of Utah, 122 South Central Campus Drive, Room 304, Salt Lake City, Utah 84112, United States

[‡]Electrochemistry Branch, Army Research Laboratory, 2800 Powder Mill Road, Adelphi, Maryland 20783, United States

[§]Wasatch Molecular Inc., 825 North, 300 West, Salt Lake City, Utah 84103, United States

Supporting Information

ABSTRACT: Molecular dynamics simulations of *N*-methyl-*N*-propylpyrrolidinium (pyr_{13}) bis(trifluoromethanesulfonyl)-imide (Ntf_2) ionic liquid [pyr_{13}][Ntf_2] doped with [Li][Ntf_2] salt and mixed with acetonitrile (AN) and ethylene carbonate (EC) organic solvents were conducted using polarizable force field. Structural and transport properties of ionic liquid electrolytes (ILEs) with 20 and 40 mol % of organic solvents have been investigated and compared to properties of neat ILEs. Addition of AN and EC solvents to ILEs resulted in the partial displacement of the Ntf_2 anions from the Li^+ first coordination shell by EC and AN and shifting the Li−Ntf_2 coordination from bidentate to monodentate. The presence of organic solvents in ILE has increased the ion mobility, with the largest effect observed for the Li^+ cation. The Li^+ conductivity has doubled with addition of 40 mol % of AN. The Li^+−N^{Ntf2} residence times were dramatically reduced with addition of solvents, indicating an increasing contribution from structural diffusion of the Li^+ cations.

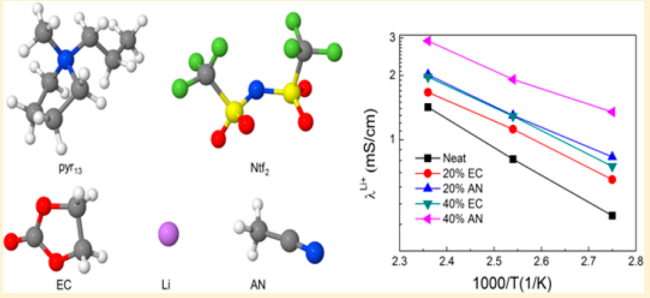

I. INTRODUCTION

Remarkable developments in the performance of lithium ion batteries have led to their extensive usage in portable electronic devices and transportation applications. Their high voltage and high energy density as compared with other rechargeable battery systems make them attractive power sources for application in variety of portable devices as well as for automotive application such as electric, hybrid-electric and plug-in hybrid-electric vehicles. However, the use of organic solvent-based electrolytes complicates application of large-scale lithium ion batteries in electric vehicles due to electrolyte volatility and flammability, which can easily lead to local overheating and eventually fire or explosion under abuse conditions. Therefore, less volatile electrolytes are highly desired for the development of electric vehicles. Ionic liquids (ILs) got significant attention due to a range of desirable properties such as nonflammability, high conductivity and electrochemical stability, and negligible vapor pressure.[1−4]

Although progress has been made in IL-based electrolytes (ILEs), their principal drawbacks, namely a relatively high viscosity and, hence, low ion diffusivity/conductivity as well as poor ability to form stable solid/electrolyte interphase on graphite anode, still hinder the commercial development of ILEs for lithium ion batteries. To overcome these barriers, researchers are focusing on synthesizing low viscosity ILs and/or use of low viscosity cosolvents.[5,6] However, designing new ILs with low viscosity that are suitable for lithium ion batteries has proven to be difficult.[7] Therefore, mixing ILEs with conventional organic solvents as thinning additives/cosolvents is considered as immediate practical solution. ILEs containing organic solvents up to 20 mol %[8] and up to 60% volume fraction[3] have been shown to retain the nonflammability. Moreover, it has been reported that organic solvent cosolvents can effectively prevent the decomposition of ILs on the negative electrode and improve reversible lithium deposition/dissolution.[9] Organic carbonates, ethers and nitriles have been examined as additives to ensure the formation of stable SEI (solid electrolyte interface) which can prevent the reduction of organic cations in ILEs.[10,11]

Mixing of ILEs with organic solvents also shows potential to improve transport properties of ILEs not only due to reduction of viscosity but also due to possible changes of Li^+ solvation structure and transport mechanisms.[6,12] It was observed that in ILEs comprised of *N*-methyl-*N*-propylpyrrolidinium(pyr_{13})/bis(trifluoromethanesulfonyl)imide(Ntf_2) IL and [Li][Ntf_2] salt (i.e., [pyr_{13}][Ntf_2]/[Li][Ntf_2]) dilution with vinylene carbonate (VC), ethylene carbonate (EC), tetrahydrofuran (THF), and toluene solvents can enhance the ion mobility. Importantly, it has been suggested that viscosity effect is not the only factor contributing to the enhanced Li^+ mobility; the changes in the Li^+−Ntf_2 association in the ILEs also play an

Received: October 22, 2014
Revised: January 2, 2015
Published: January 16, 2015

DOI: 10.1021/jp510644k
J. Phys. Chem. B 2015, 119, 3085−3096

important role. Addition of 20 mol % EC into the $[pyr_{13}][Ntf_2]$/$[Li][Ntf_2]$ electrolyte resulted in reduction of the ILE viscosity almost by a factor of 2 compared to undiluted ILE. However, the self-diffusion coefficient of ions did not increase proportionally to viscosity reduction, indicating a change in the conduction mechanism or availability of the charge carriers. While the self-diffusion coefficient of Li^+ increased the most compared to other ions, it only increased by a factor of 1.6 compared to pure ILE. Addition of 20 mol % tetraglyme into $[pyr_{13}][Ntf_2]$/$[Li][Ntf_2]$ electrolytes was able to reduce viscosity (by a factor of 2.1) as well as to increase conductivity (by a factor of 1.9) and self-diffusion coefficients of pyr_{13} (by a factor of 2.5) and Ntf_2 (by a factor of 3.5) compared to the values observed in the pure $[pyr_{13}][Ntf_2]$ at different temperatures.[13] However, the Li^+ diffusion increased by as much as factor of 4 upon addition of tetraglyme, again indicating that the viscosity of ILE is not the only factor in determining Li^+ mobility.

Raman spectroscopy provided an additional insight into the changes in the Li^+ cation solvation shell composition upon ILEs dilution with organic solvents. For example, in the Raman analysis of [1-methyl-3-ethylimidazolium (emim)][Ntf_2] doped with $[Li][Ntf_2]$ salt and diluted with EC, VC,[14] or oligoethers,[15] the researchers associated the Ntf_2 $\delta_s CF_3$ mode located at 742 cm^{-1} with "free" Ntf_2 and the mode around 748 cm^{-1} with Ntf_2 directly interacting with Li^+. Lassègues et al.[15−17] interpreted changes of IL Raman and IR spectrum as a function of $[Li][Ntf_2]$ concentration as formation of $[Li^+(Ntf_2)_2]^-$ clusters. When oligoethers were added to $[emim][Ntf_2]$/$[Li][Ntf_2]$ intensity of the "free" Ntf_2 band increased, indicating that oligoethers dissolved the $[Li^+(Ntf_2)_2]^-$ complexes and Li^+(oligoether) solvates formed in the electrolytes.[15] Similarly, Hardwick et al.[14] found that addition of 2 M EC and VC to $[emim][Ntf_2]$/0.5M$[Li][Ntf_2]$ also increased the magnitude of the "free" 742 cm^{-1} Ntf_2 peak and eliminated the 748 cm^{-1}. This conclusion was consistent with the appearance of the blue-shifted band for EC ring breathing mode that occurs during EC direct complexation with Li^+. The coordinated IR and Raman and DFT study of the $[Li][Ntf_2]$-containing ILs indicated that at low salt concentrations the $[Li^+(Ntf_2)_2]^-$ clusters prevail, while the $[Li^+(Ntf_2)_4]^{3-}$ clusters yield a negligible contribution.[16] In the follow up study of $[Li][Ntf_2]$ in $[pyr_{14}][Ntf_2]$, they reported that the concentration dependence of the average number of Ntf_2 anions coordinating to one Li ion ($N_{Ntf2/Li}$) can be divided into three regimes: $x \leq 0.05$, $0.1 \leq x \leq 0.2$ and $x > 0.2$, where x is the lithium salt mole fraction.[17] At low concentraions a large number of Ntf_2 anions coordinate each Li ion. At intermediate concentrations, the $[Li(Ntf_2)_2]^-$ clusters prevail, while at higher concentrations, aggregates with bridging Ntf_2 anions were found. A recent DFT study[18] of acetonitrile $[(AN)_m\ Li(Ntf_2)_n]^{(n-1)-}$ solvates showed that the 742 cm^{-1} band exhibits a blue shift by 5−8 cm^{-1} due to bidentate binding of Li^+ to Ntf_2 oxygen atoms. However, the DFT studies of the $[(AN)_3\ Li(Ntf_2)]$ complexes with monodentate Li^+-O^{Ntf2} coordination were found to be more energetically stable than the bidentate analogues in the gas phase. Interestingly, Raman $\delta_s CF_3$ band in the $[(AN)_3\ Li(Ntf_2)]$ complexes with monodentate binding of O^{Ntf2} to Li^+ exhibit very minor blue shift (0−3 cm^{-1}) compared to the one observed for complexes with the bidentate Li^+-Ntf_2 binding. A bidentante and monodentante coordination of Li^+ with Ntf_2 are illustrated in Figure 1. This observation suggested a possibility that the $[Li(Ntf_2)_n]^{(n-1)-}$ complexes with the monodentate binding could have been counted as "free" Ntf_2 anions during interpretation of the Raman spectrum, therefore challenging the conclusion of the

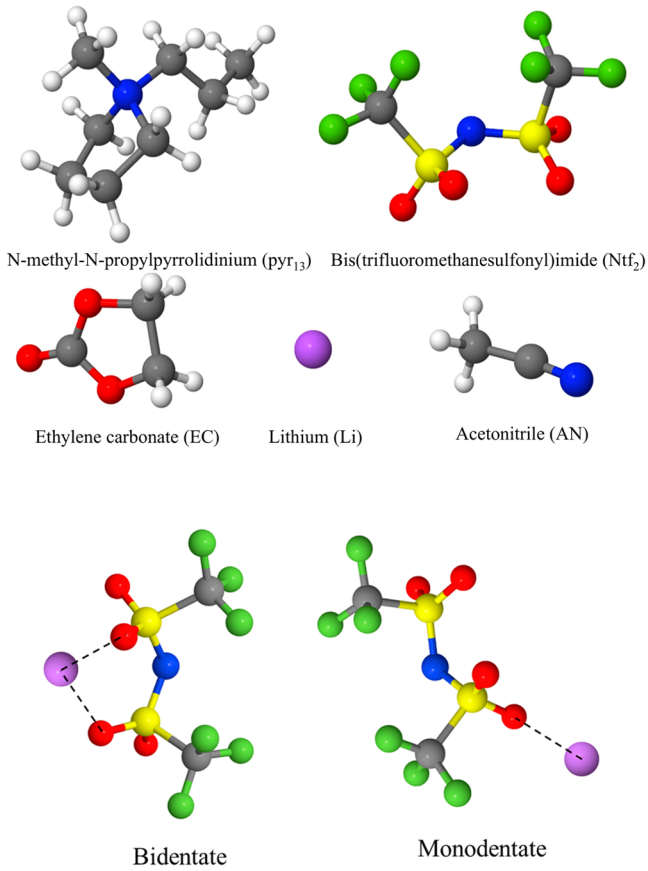

Figure 1. Chemical structure of compounds comprising investigated ILEs. Also shown are configurations of monodentate and bidentate Li−Ntf_2 coordination.

$[Li^+(Ntf_2)_2]^-$ complexes being the dominant in these ILEs. While the Raman spectroscopy certainly provides valuable data for characterizing the coordination environment of ions in ILEs,[6,14,15,19,20] the interpretation of influence of organic solvents on these environments in ILEs can be complicated.

Although the above-mentioned studies provided some insight into the Li^+ solvation structure and transport in mixed ILEs, the liquid structure and details of the Li^+ coordination as well as the role of organic cosolvents in such ILEs are still not fully understood. Li^+ cations in ILEs can move together with their coordination shell (vehicular mechanism) or by exchanging coordinated molecules in the shell (structure diffusion mechanism).[21] The addition of solvent can affect both of these mechanisms.

Molecular dynamics (MD) simulation is a promising research tool for studying ILEs and their mixtures with lithium salts and/or organic solvents as it allows to access the details of ion coordination and transport mechanisms, provided that the force field adequately represents ionic interactions.[21−23] The many-body polarizable APPLE&P force field for *N*-methyl-N-propylpyrrolidinium$[pyr_{13}]$ cations, Ntf_2 anion, including the interactions of Ntf_2 with Li^+, and various organic solvents has been developed and validated in our previous works.[24−31] The $[pyr_{13}][Ntf_2]$ IL doped with 25 mol % $[Li][Ntf_2]$ was first studied by MD simulations using the developed force field.[21] Using this force field, a recent simulation study of the influence of lithium salt concentration on structural and transport properties of $x[Li][Ntf_2]/(1-x)[pyr_{13}][Ntf_2]$ electrolytes also showed accurate prediction of ion self-diffusion coefficients and ionic

DOI: 10.1021/jp510644k
J. Phys. Chem. B 2015, 119, 3085−3096

conductivity compared to experiments.[32] These studies showed that Li^+ cation in the electrolyte is coordinated on average by ~3.3 Ntf_2 anions that contribute about 4.1 O atoms to the Li^+ first coordination shell. The APPLE&P force field has been recently validated for acetonitrile $[(AN)_m\ Li(Ntf_2)_n]^{(n-1)-}$ and $[Li^+(Ntf_2)_2]^-$ complexes by comparing cluster geometries and binding energies obtained from molecular mechanics optimizations with quantum chemistry calculations.[18] MD simulations using this APPLE&P force field were also conducted to examine the Li^+ solvation structure and ionic association in the AN/$[Li][Ntf_2]$ mixtures.[18]

In this paper, the previous study of neat $[pyr_{13}][Ntf_2]$/$[Li][Ntf_2]$ ILEs[32] was extended to ILEs diluted with AN and EC organic cosolvents using a modified APPLE&P force field.[33] In the modified force field, the polarizability of the Ntf_2 anion oxygen atom was reduced from 1.36 to 1.00 Å^3, allowing a more accurate prediction of the binding energy of the $[Li(Ntf_2)_n]^{(n-1)-}$ complexes.[33] EC or AN solvents were added to the neat electrolyte $0.16[Li][Ntf_2]/0.84[pyr_{13}][Ntf_2]$. EC is often used as a prime constituent in organic electrolytes for lithium ion batteries and is known to play an important role in formation of stable SEIs at anode surface. Moreover, bulk EC has a large dielectric constant (~90) which promotes ions dissociation and has an acceptable viscosity (1.9 cP at 40 °C) that fosters ion diffusion. As a low-viscosity aprotic liquid, AN has been shown to considerably enhance the ionic mobility in $[pyr_{1x}][Ntf_2]$ ILE.[28] AN mixed with lithium salts has shown to have good conductivity and strong permittivity.[34] Solvation interactions of AN molecules with ions are relatively straightforward due to a single electron lone-pair in AN molecule. The lone-pair allows AN to coordinate only with a single Li^+ cation.

To the best of our knowledge, there has been only one reported MD simulation study of $[pyr_{13}][Ntf_2]/[Li][Ntf_2]$/organic solvent ILEs using a nonpolarizable force field.[35] In that work, investigators reported an enhancement of Li^+ mobility in the ILE due to presence of EC, VC, and THF. Although that simulation reported electrolyte densities and the Li^+ self-diffusion coefficients that agreed with experimental data, the Li^+ coordination structure predicted from those simulations appears to contradict with previous quantum chemistry calculations of $[Li(Ntf_2)_n]^{(n-1)-}$ clusters as well as experiments and simulations of neat $[pyr_{13}][Ntf_2]/[Li][Ntf_2]$. The force field used in that work seems to significantly favor the interaction between Li^+ and the N atoms of Ntf_2 instead of O atoms, which is clearly evident by a strong peak in the radial distribution functions at short (~2 Å) distance.[35] Latest high-level DFT calculations using complete basis set extrapolation at MP2 level[25] indicate that $Li-N^{Ntf2}$ binding is more than 10 kcal/mol less favorable than the $Li-O^{Ntf2}$ binding. Also no such close approaches between Li and N^{Ntf2} were observed in our previous simulations of the same system using polarizable force field[32] as well as it appears to contradict the experimental analysis discussed above of mono- and bidentate arrangement of Ntf_2 anions around Li^+. Therefore, MD simulations using the APPLE&P force field reported here will focus on understanding the influence of organic solvents on Li^+ solvation and ion transport properties. For comparison purpose, the pure organic solvents and neat $0.16[Li][Ntf_2]/0.84[pyr_{13}][Ntf_2]$ systems were also analyzed in this work.

II. MOLECULAR DYNAMICS SIMULATION METHODOLOGY

In this work, all MD simulations were performed using the atomistic many-body polarizable force field APPLE&P. This force field has been extensively validated for various ILs, including those containing $[Li][Ntf_2]$ salts, as well as for variety of organic electrolytes with various lithium salts.[24−27] Recently, it was noted that M05-2X density functional, which was used for parametrization of the force field ability to describe the Li-Ntf_2 binding energy, significantly overestimates this energy.[33] Such overestimation of the binding energy resulted in a slower Li^+ diffusion in the Ntf_2-based ILs.[29] Thus, the force field was refitted to Li-Ntf_2 binding energy obtained from the more accurate G4MP2 composite methodology by reducing polarizability of the Ntf_2 oxygen atom from 1.36 Å^3 to 1.0 Å^3.[33] The G4MP2 results agreed well with the complete basis set extrapolation of the MP2 binding energy.[25] Reduction of the Li-Ntf_2 binding energy resulted in an improved agreement for the Li^+ solvation number in EC/$[Li][Ntf_2]$ as a function of salt concentration between MD simulations and Raman spectroscopy[33]

The in-house developed MD simulation package that can handle many-body induced polarization interactions was used for all MD simulations. Compositions of the investigated systems are summarized in Table 1 while chemical structure of ions and solvents is shown in Figure 1. The mixtures of neat $0.16[Li][Ntf_2]/0.84[pyr_{13}][Ntf_2]$ ILE with 20 and 40 mol % EC or AN were simulated in the 363−423 K temperature range and atmospheric pressure. Initially each electrolyte was mixed at 500 K and then cool down to the desired temperature. Starting configurations of electrolytes for lower temperatures were taken from equilibrated configurations at the closest higher temperature.

Table 1. Number of Molecules Comprising Each ILE System Investigated

systems						
		pyr_{13}	Ntf_2	Li	EC	AN
20 mol %	EC	124	148	24	32	–
	AN	124	148	24	–	32
40 mol %	EC	124	148	24	96	–
	AN	124	148	24	–	96

All simulations were conducted using the multiple-time step integration scheme proposed by Martyna et al.[36,37] that allowed us to control the temperature and pressure with the associated frequencies of 10^{-2} and 0.5×10^{-3} fs, respectively. Bond lengths were constrained using the Shake algorithm[38] to allow utilization of a larger time step. The long-range electrostatic forces, including forces between partial charges with partial charges and partial charges with induced dipoles, were treated using the Ewald summation method. The induced dipole−induced dipole interactions were scaled to zero at a cutoff distance of 11.0 Å by a tapering function, with the scaling starting at 10.2 Å. A time step of 0.5 fs was used for bonds, bends, and out-of-plane deformations, a 1.5 fs for torsions and for nonbonded interactions within a 6.5 Å (EC diluted system) or 7.0 Å (all other systems) cutoff radius, and a 3.0 fs step for nonbonded interactions between 6.5 or 7.0 and 11.0 Å and the reciprocal part of the Ewald summation. All systems were first simulated in the *NPT* ensembles for at least 6 ns to establish equilibrium density.

DOI: 10.1021/jp510644k
J. Phys. Chem. B 2015, 119, 3085−3096

Then, production runs in the *NVT* ensemble were conducted over 25 ns for all systems.

III. RESULTS AND DISCUSSION

A. Neat ILE. A detail analysis of structural and transport properties of neat $x[Li][Ntf_2]/(1-x)[pyr_{13}][Ntf_2]$ ILEs as a function of Li salt content and temperature has been presented in our previous work.[32] However, as we pointed above, we have utilized the revised description of the Ntf_2 anion and have used reduced polarizability for oxygen atoms. Therefore, it is instructive to briefly discuss how this force field modification affected the properties of neat ILE. For this purpose we compared the simulations of $0.16[Li][Ntf_2]/0.84[pyr_{13}][Ntf_2]$ at several temperatures using both force fields. Adjustment of the force field had only minor influence on most of the properties. For example, the changes for ionic conductivity were less than 10% which is comparable to the statistical uncertainty of our data for this property. Similarly, the changes in self-diffusion coefficients of ions and viscosity were on the order of 10−20%. However, the structural correlations involving Li^+ showed more noticeable changes. First, in simulations with the new force field the number of Ntf_2 oxygen atoms in the Li^+ coordination shell increased from 4.1 to 4.8 oxygens for this ILE at 363 K. However, the number of coordinating nitrogen atoms reduced from 3.5 to 3.1, indicating that in simulations with the new force field we have an increased amount of Ntf_2 anions that have bidentate binding to the Li^+ and are contributing about two oxygen atoms into Li^+ first coordination shell. This change is clearly illustrated in Figure 2 where the Li^+−N radial distribution functions are

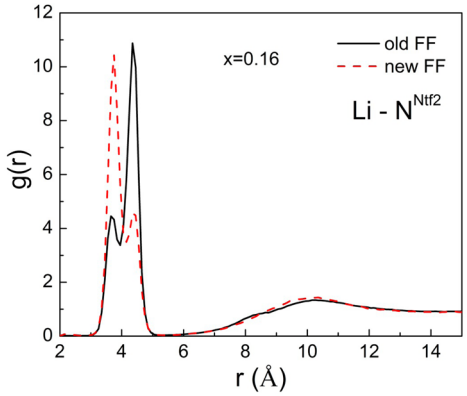

Figure 2. $Li-N^{Ntf2}$ radial distribution function obtained from simulations of $0.16[Li][Ntf_2]/0.84[pyr_{13}][Ntf_2]$ ILE at 363 K using old and revised force fields.

compared for simulations of $0.16[Li][Ntf_2]/0.84[pyr_{13}][Ntf_2]$ at 363 K using both force fields. As we discussed in our previous work, this distribution function has two maxima in its first peak; the first one is due to anions that have bidentate orientation while the second one (at further distances) is from anions that are in monodentate orientation. Figure 2 clearly shows that the new force field noticeably changes the relative population of these orientations and is more consistent with those experimental data that suggest the dominance of the bidentate binding of Ntf_2 anions to Li^+ in ILEs.[15,22,39] Note that the issue of how many Ntf_2 anions are coordinating Li^+ in neat ILEs is an ongoing debate. While some researchers[16,17] interpret their experimental data as a definitive indication of formation of $[Li^+(Ntf_2)_2]^-$ complexes (and hence exclusively the bidentate binding of anions to Li^+), others see evidence of formation of $[Li^+(Ntf_2)_3]^{2-}$ and $[Li^+(Ntf_2)_4]^{3-}$ complexes[14,40−42] indicating the presence of monodentate anions in the Li^+ coordination shell. As we discussed above the interpretation of Raman measurements might be complicated due to absence or overlap of distinct signatures of certain species in the spectral data. Simulations with the new force field predict that about 50% of anions coordinating Li^+ are in bidentate configuration.

Another, noticeable difference is in the Li^+−Li^+ pair distribution functions. Simulations using the old force field have predicted a formation of small Li^+ clusters in ILEs with low concentrations of Li salt.[43] Figure 3 illustrates this trend by

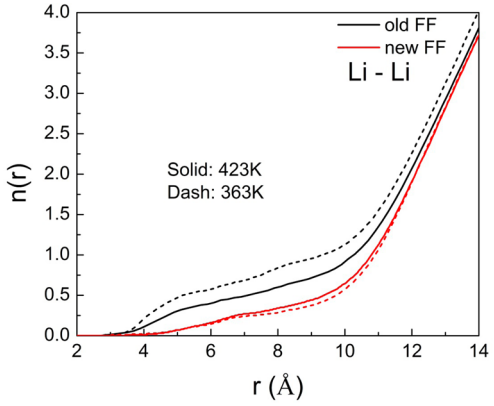

Figure 3. Li^+−Li^+ coordination number as a function of shell radius as obtained from simulations of $0.16[Li][Ntf_2]/0.84[pyr_{13}][Ntf_2]$ ILE at 363 K using the old and revised force fields.

showing the Li^+−Li^+ cumulative coordination numbers and indicating that in simulations with the old force field there are about 0.5−0.6 Li^+ neighbors within the 6 Å radius shell of every Li^+. However, to reach the same number of neighbors in simulations with the new force field the shell has to be extended to about 9 Å, which corresponds to a random distribution of Li^+ in the system. Therefore, while simulations using the old force field were showing some Li^+ clustering, the new force field shows almost homogeneous distribution of Li^+ in neat ILE. This comparison of two force fields illustrates that subtle changes in the polarization interactions (the two force fields differ only by slight change of polarizability parameter for in Ntf_2 oxygen atoms) can noticeable affect Li^+ local environment. Yet, the transport properties of the neat ILE seem to be unaffected by these structural changes and force field parameters, at least in the investigated temperature range.

The discussed above results clearly indicate a complex interplay and sensitivity between the force field parameters and properties predicted by MD simulations using parametrized force fields. While some properties might be insensitive to force field parameters, others will have a much stronger sensitivity and hence, a careful validation/refinement of the force field against quantum chemistry calculations and experiments are needed. In the remaining of the paper we will only discuss the results obtained using the new force field.

B. Structural Properties. *ILEs Structure.* Densities of the investigated electrolytes obtained from MD simulations are listed in Table 2 along with available experimental measurements. Densities of pure EC or AN solvents and neat $0.16[Li][Ntf_2]/0.84[pyr_{13}][Ntf_2]$ ILE are also shown for comparison. As we can see from Table 2, addition of 20 mol % of organic solvents does not lower the densities of the ILEs significantly. If we would

DOI: 10.1021/jp510644k
J. Phys. Chem. B 2015, 119, 3085−3096

Table 2. Density (ρ, kg/m^3) of Investigated ILEs and Pure Solvents at Different Temperatures As Obtained from MD Simulations[a]

			0.16[Li][Ntf_2]/0.84[pyr_{13}][Ntf_2] ILE				
				with solvent			
T (K)	EC	AN	neat	20% EC	20% AN	40% EC	40% AN
423	1175	650	1376	1366	1349	1349	1298
				(1336)	(1231)	(1296)	(1086)
393	1272	661	1415	1408	1392	1375	1325
				(1388)	(1266)	(1359)	(1115)
363	1252	700	1442	1434	1417	1403	1352
				(1404)	(1294)	(1366)	(1145)
313	1303	756					
313 (exp)[51,52]	1317	759					
293 (exp)[6]			1470	1470			

[a]Also listed are available data from experiments. Data in parentheses are the values estimated assuming ideal mixing of neat 0.16[Li][Ntf_2]/0.84[pyr_{13}][Ntf_2] and organic solvents at corresponding temperature. Error bars for reported densities are less than 1%.

assume that these solvents mix with neat ILE ideally we should've obtained much lower densities that are shown in parentheses, especially for ILEs containing AN. The observed limited (compared to ideal mixing values) reduction in densities of diluted ILEs indicates a much more efficient packing of solvent molecules in the ILE than in ideal mixtures. Interestingly, the deviation between the ideal mixing and real densities for EC diluted ILEs is significantly less than for ILEs containing AN, indicating that AN molecules are more efficient in packing between ions compared to EC and that perhaps more AN molecules can be involved in the Li^+ first coordination shell. These results are in accord with observed significantly more negative excess volume values for [pyr_{1S}][Ntf_2]/AN mixture compared to [pyr_{1S}][Ntf_2]/propylene carbonate(PC) (or EC) mixtures obtained from experiments[44] and simulations.[28]

The structure of ILEs can be characterized through examination of various radial distribution functions (RDFs) between the species comprising it. In Figure 4 we examine RDFs

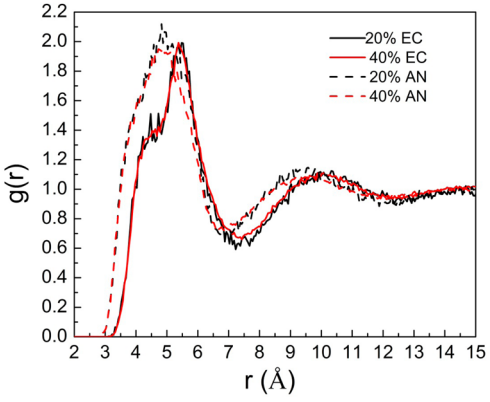

Figure 4. EC-EC and AN-AN center-of-mass radial distribution functions (RDFs) as obtained from MD simulations of ILEs at 363 K.

for the solvent molecules centers-of-mass. The small value of the peaks in the center-of-mass RDFs for EC−EC and AN−AN indicates that solvent molecules are well dispersed in the ILEs and have very little tendency for clustering. This is consistent with the observation that both of these solvents have a good solubility in neat ILs comprised of this type of cation and Ntf_2 anion. The solvent RDFs shown in Figure 4 are similar to those obtained in IL/solvent mixtures not containing Li salts.[28]

Li^+ Coordination Shell. It has been reported that Li^+ can be strongly coordinated by oxygen atoms from Ntf_2 anions (O^{Ntf2}),[21] carbonyl oxygen atoms (O_c^{EC}) from EC[45] and nitrogen atoms from AN (N^{AN}).[18] We have examined the Li^+-O^{Ntf2}, $Li^+-O_c^{EC}$, and Li^+-N^{AN} RDFs and found strong peaks in the RDFs at short separations (see Figures SI.1 and SI.2 in the Supporting Information) indicating that the Li^+ cations are closely coordinated by O atoms from Ntf_2 and EC as well as by the N atoms from AN. However, the coordination by two solvents has different composition dependence. While for mixtures with EC the first peak in the RDF is almost unchanged with increase of EC concentration, the peaks for Li^+-N^{AN} RDFs show noticeable reduction with increasing concentration of AN indicating that the solvent chemical structure can noticeably influence the composition dependence of the Li^+ solvation in mixed ILEs. Finally, the fact that the position of peaks in $Li^+-O_c^{EC}$ and Li^+-N^{AN} RDFs were at the same distance as the peaks in Li^+-O^{Ntf2} RDFs indicate that both solvents are present in the first coordination shell of Li^+ cations in the investigated ILEs.

Using these RDFs we have characterized the coordination shell of Li^+ by calculating the cumulative Li^+ coordination numbers by carbonyl oxygen of EC, oxygen atoms of Ntf_2, and the nitrogen atoms of AN and Ntf_2. The number density-weighted integrals of RDFs yielded the cumulative coordination numbers shown in Figure 5 for investigated ILEs at 363 K. In agreement with previous reports,[22,46] the temperature dependence of these coordination numbers is very weak and thus the results for other temperatures are not shown. On the basis of the Li^+-O^{Ntf2}, $Li^+-O_c^{EC}$, and Li^+-N^{AN} RDFs, we can define the first coordination shell of Li^+ as a shell with a radius of r = 3.0 Å, i.e., the position of the first minimum in RDFs. As can been seen from Figure 5a, in the neat ILE the Li^+ cations are, on average, coordinated by 4.8 O^{Ntf2} atoms. As expected, upon addition of organic solvents, the Li^+-O^{Ntf2} coordination number is reduced, with more reduction observed in the AN diluted ILEs. There are on average 4.5 O^{Ntf2} atoms around a Li^+ in the ILE with 20% EC and 3.9 in ILE containing 20% AN. Addition of more organic solvent into ILEs continues to reduce the number of O^{Ntf2} atoms around Li^+ cations. Reductions of 0.8 and 1.9 are obtained in 40 mol % EC and AN electrolytes, respectively, indicating that AN replaces the Ntf_2 anions to a larger extent than EC.

Since the organic solvent molecules can only contribute one coordinating atom (O_c or N), the number of O_c^{EC} and N^{AN} coordinating Li^+ cations must represent the number of molecules around Li^+. As shown in Figure 5b, within a 3.0 Å shell, there are

DOI: 10.1021/jp510644k
J. Phys. Chem. B 2015, 119, 3085−3096

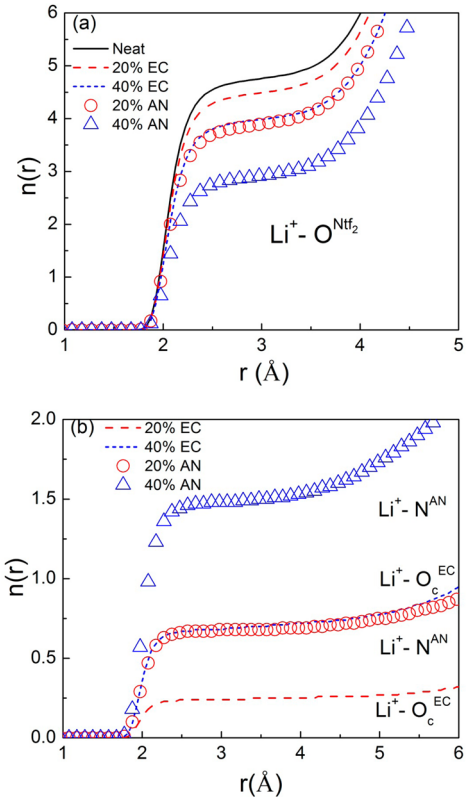

Figure 5. Cumulative coordination number of Li^+ by (a) the oxygen atoms from Ntf_2 anions and (b) the carbonyl oxygen atoms from EC and the nitrogen atoms from AN.

on average 0.2 and 0.7 O_c^{EC} atoms around a Li^+ cation in the 20 and 40 mol % EC electrolytes, respectively. The number of N^{AN} atoms within Li^+ first coordination shell, however, is 0.7 and 1.5 in the 20 and 40% AN electrolytes, respectively. This implies that, at the same extent of dilution, AN molecules have more ability to replace Ntf_2 anions in the Li^+ coordination than EC molecules.

Next we analyze the probability distribution of finding a certain number of O^{Ntf2} in the Li^+ coordination shell as shown in Figure 6 for the neat and diluted ILEs in order to understand the extent of instantaneous fluctuations of the Li^+ local environment composition. A broad distribution of the Li^+ coordination environments has been observed, with Li^+ cations being coordinated by as much as 6 and as few as 0 or 1 O^{Ntf2} atoms.

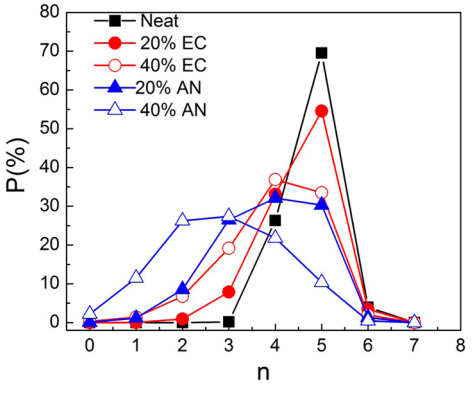

Figure 6. Distribution of instantaneous Li^+–O^{Ntf2} coordination numbers within the first coordination shell of Li^+ in neat and diluted ILEs.

Occasionally, a Li^+ cation is coordinated by seven O^{Ntf2} atoms, but the probability of these events is very small. In the neat ILE, Li^+ cations are coordinated mainly by 4 or 5 O^{Ntf2}, therefore, resulting in an average coordination number of 4.8. The observed 4- and 5-fold coordination structures agree well with those reported in previous MD simulations and experiments.[23,22] As 20 mol % of EC is added to ILE, the distributions are shifting to the left with reduction of probability for the 5-fold coordination and an increase for the 3- and 4-fold coordination structures. As the EC concentration is increased to 40 mol % further shift to the left and appearance of 1- and 2-fold coordinations are observed, in particular, the 5-fold coordination is no longer the predominant structure. Interestingly, the probability of finding the 4-fold coordination is almost not changing upon addition of more EC. Addition of 20% AN results in the distribution of O^{Ntf2} environments of Li^+ very similar to that observed for 40% EC ILE, i.e., the most probable being the 4-fold coordination. Further dilution with AN makes the distribution very broad, ranging from 0- to 6-fold coordinations with the 3-fold coordination being the most probable.

Next we examine the influence of added solvent on the details of Li^+–Ntf_2 coordination. Since there is only one N atom in the Ntf_2 anion, the coordination numbers for Li^+–N^{Ntf2} can be very useful in this analysis. As has been shown in Figure 2 and also shown in Figure SI.3, the Li^+–N^{Ntf2} RDF has the first peak splitted into two, with the first maximum corresponding to bidentate orientation of anion and the second to monodentate. Therefore, the location of the minimum at 4.1 Å that separates the two maxima in the Li^+–N^{Ntf2} RDF can be considered as the boundary differentiating the bidentate and monodentate orientations Ntf_2, while r = 5.3 Å defining the total first coordination shell of anions around Li^+. Figure 7 shows the Li^+–

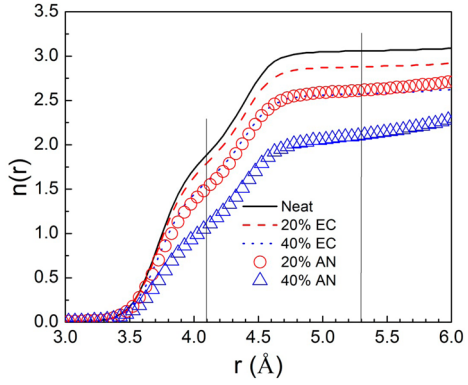

Figure 7. Li^+–N^{Ntf2} cumulative coordination number of N^{Ntf2} as a function of separation from Li^+.

N^{Ntf2} cumulative coordination numbers for the neat and diluted ILEs. This figure shows that there are on average three N^{Ntf2} atoms binding to a Li^+ cation in the first coordination shell in the neat electrolyte. Upon addition of organic solvents, the average N^{Ntf2} coordination number drops to as low as 2 in 40% AN ILE. Figure 8 plots the probability distributions of the number of N^{Ntf2} near Li^+. In the neat ILE, about 90% of Li^+ cations have three anions within their first coordination shell. This fraction, however, lowers to 77% and 57% in 20% EC and 20% AN electrolytes, respectively, and continues to decrease as more organic solvents is added. At the same time, the fraction of Li^+ cations coordinated by two anions increases from 2.5% to 51.6% in the 40% AN electrolyte and the $[Li^+(Ntf_2)_2]^-$ complex

DOI: 10.1021/jp510644k
J. Phys. Chem. B 2015, 119, 3085−3096

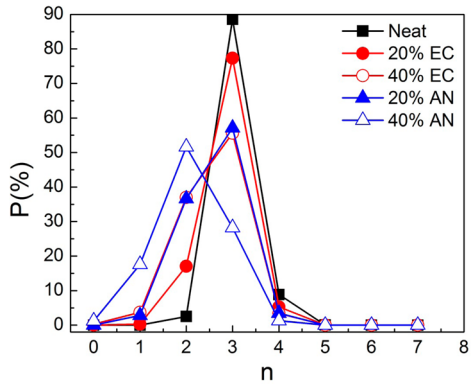

Figure 8. Probability of finding certain Li^+-N^{Ntf2} coordination number in neat and diluted ILEs.

becoming the most probable one. This observation again supports that the organic solvents are capable to scavenge the Li^+ cations away from the Ntf_2 anions, especially the AN solvent. The value of the cumulative coordination number at $r = 4.1$ Å in Figure 7 shows the average number of bidentate anions. In the neat ILE, Li^+ on average has about equal amount of Ntf_2 anions in the bidentate and monodentate orientation, ~1.5 anions of each type per Li^+. With addition of solvent the amount of bidentate anions is reducing. The reduction of bidentate anions can be either due to complete replacement of these anions by EC or AN molecules, i.e., changing $[Li^+(Ntf_2)_n]^{(n-1)-}$ to $[Li^+(Ntf_2)_{(n-1)}\text{solvent}]^{(n-2)-}$ complexes, or due to conversion of bidentate anions to monodentate coordination, allowing EC or AN molecule to coordinate Li^+ cation and forming a $[Li^+(Ntf_2)_n\text{solvent}]^{(n-1)-}$ complex. Note that in the latter scenario, the total number of anions within the first coordination shell of a Li^+ would not change, but the number of O^{Ntf2} atoms would reduce. However, Figure 7 clearly shows that within the 5.3 Å shell, which is the location of the second minimum in the Li^+-N^{Ntf2} RDF and hence defines the first coordination shell of anions around Li^+, the overall reduction in Li^+-N^{Ntf2} coordination number is even somewhat larger than the reduction in the number of bidentate anions (n, at r =4.1 Å). This implies that upon addition of solvent molecules the Li^+ cations are losing monodentate anions as well. Table 3 reports the average

Table 3. Average Number of Bidentate, Monodentate, and Total Ntf_2 Anions Coordinating Li^+ in the Neat and Diluted ILEs As Obtained from MD Simulations at 363 K

system	bidentate	monodentate	$n(N^{Ntf2})$
neat	1.6	1.4	3.0
20% EC	1.5	1.4	2.9
40% EC	1.4	1.1	2.5
20% AN	1.3	1.3	2.6
40% AN	0.8	1.3	2.0

numbers of bidentate, monodentate and the total of anions in the first coordination shell of Li^+. This table clearly shows that both the total number of anions and bidentate orientation are reducing noticeably with addition of the solvent, yet the average number of monodentate stays almost the same. The latter effect is due mutual compensation between the replacement (by solvent) of monodentate anions and the conversion of bidentate into monodentate orientations.

The details of changes in the Li^+ solvation structure can be also quantified by calculating contributions of different $[Li^+(Ntf_2)_n]^{(n-1)-}$ complexes to each Li^+-O^{Ntf2} coordination structure $[Li^+(O^{Ntf2})_k]$. For example, a 5-fold Li^+-O^{Ntf2} coordination ($[Li^+(O^{Ntf2})_k]$, $k = 5$) can, in principle, be comprised of two, three, or more Ntf_2 anions ($n = 2$, 3, 4, etc.). The relative populations of these different environments are summarized in Table 4 for each investigated ILE. In the neat ILE Li^+ cations are mainly coordinated by four or five O^{Ntf2} atoms (5-fold and 4-fold rows in Table 4). For these clusters the majority of complexes contain three (n=3) Ntf_2 anions. For the 5-fold/3-anions clusters ($k = 5$, $n = 3$), the two anions are in bidentate orientation and the third one is a monodentate. In the ($k = 5$, $n = 4$) clusters, there are three monodentate and one bidentate anions. As the dilution of ILE with EC and AN solvents increases, we can see a significant reduction in the number of clusters with large k (i.e., the number of O^{Ntf2} atoms) and n (number of anions) values in the Li^+ coordination. Instead, complexes with smaller numbers of O^{Ntf2} atoms ($k = 3$ and 2) and anions ($n = 1$ and 2) become more populated. This trend is consistent with discussed above elimination of bidendate orientation upon addition of solvent. This analysis indicates that in diluted electrolytes the Li^+ cations tend to have less Ntf_2 anions involved in their first coordination shell, which should benefit the Li^+ transport which is analyzed in the next section.

C. Transport Properties. *Self-Diffusion Coefficients.* The self-diffusion coefficient D_i of component i was calculated using the Einstein relation

$$D_i = \lim_{t\to\infty} D_i^{app}(t) = \lim_{n\to\infty} \frac{\langle \mathrm{MSD}_i(t)\rangle}{6t} \quad (1)$$

where $\mathrm{MSD}_i(t)$ is the mean-squared displacement of the center-of-mass of a component i after time t, $\langle\ \rangle$ denotes an ensemble average. The self-diffusion coefficients obtained from MD simulations for each ILE component are plotted as a function of temperature in Figure 9. For the neat and 20% EC ILEs the available experimental data at 293 K are also shown on the figure.[6,13] Given the fact that our systems have a slightly lower lithium salt concentration (about 0.60 M at 293 K) than the reported experiment data (0.65 M at 293 K), the extrapolation of simulation self-diffusion coefficients obtained at elevated temperatures to 293 K shows a good agreement with experiment for all components of ILE. The diffusivity of the ILE components follows the following order AN >EC > pyr_{13} > Ntf_2 > Li^+, which is also in agreement with experimental data. As expected, the presence of organic solvents in ILE increases the mobility of ions. The enhancement of ion self-diffusion coefficient upon solvent addition is more apparent if the ratio of self-diffusion coefficient in the diluted systems to the neat ILE is plotted as shown in Figure 10. Encouragingly, the mobility of Li^+ cation increases the most (compared to other ions) upon addition of the solvents. Mobility of Ntf_2 anions is the second most increased, probably because some Ntf_2 anions are displaced from the $Li(Ntf_2)_n$ complexes by solvent and can diffuse as uncoordinated anions. The increase of pyr_{13} mobility is the smallest, as this cation does not participate in the strongly interacting Li^+ clusters. This order of mobility increase is also in a good agreement with experimental data.[6] As has been suggested in previous works,[6,13] the reduced viscosity is not the only factor resulting in the improvement of ion mobility upon dilution of ILE with a solvent. The enhanced ion motion can be also attributed to the changes in the Li^+ cation solvation structure discussed above.

DOI: 10.1021/jp510644k
J. Phys. Chem. B 2015, 119, 3085−3096

Table 4. Population (%) of $[Li^+(Ntf_2)_n]^{(n-1)-}$ Complexes (for n = 1, 2, 3, and 4) That Contribute to k-Fold Coordination Structures of Li^+ by O^{Ntf2}[a]

		Systems				
no. of O^{Ntf2} coordinating Li^+	no. of contributing Ntf_2, n	neat	20% EC	40% EC	20% AN	40% AN
5-fold $[Li^+(O^{Ntf2})_5]$	n = 1, $[Li^+(O^{Ntf2})_5$	–	–	–	–	
	n = 2, $[Li^+(O^{Ntf2})_5]^-$	0.1	0.1	0.1	0.1	0.1
	n = 3, $[Li^+(O^{Ntf2})_5]^{-2}$	50.4	39.3	25.3	26.6	9.2
	n = 4, $[Li^+(O^{Ntf2})_5]^{-3}$	4.2	3.0	1.4	1.7	0.4
	total for 5-fold	**54.7**	**42.4**	**26.8**	**29.4**	**9.7**
4-fold $[Li^+(O^{Ntf2})_4]$	n = 1, $[Li^+(O^{Ntf2})_4]$	–	–	–	–	–
	n = 2, $[Li^+(O^{Ntf2})_4]^-$	7.2	12.9	19.2	13.8	13.6
	n = 3, $[Li^+(O^{Ntf2})_4]^{-2}$	31.8	28.3	20.8	21.3	10.4
	n = 4, $[Li^+(O^{Ntf2})_4]^{-3}$	3.2	2.4	1.0	1.3	0.3
	total for 4-fold	**42.2**	**43.6**	**41.0**	**36.4**	**24.3**
3-fold $[Li^+(O^{Ntf2})_3]$	n = 1, $[Li^+(O^{Ntf2})_3]$	-	-	<0.1	-	<0.1
	n = 2, $[Li^+(O^{Ntf2})_3]^-$	0.4	7.7	18.3	19.5	27.1
	n = 3, $[Li^+(O^{Ntf2})_3]^{-2}$	0.4	3.0	4.2	5.8	5.9
	n = 4, $[Li^+(O^{Ntf2})_3]^{-3}$	–	–	–	–	–
	total for 3-fold	**0.8**	**10.7**	**22.5**	**25.3**	**23.0**
2-fold $[Li^+(O^{Ntf2})_2]$	n = 1, $[Li^+(O^{Ntf2})_2]$	–	0.3	3.1	2.8	10.2
	n = 2, $[Li^+(O^{Ntf2})_2]^-$	<0.1	0.8	4.0	4.7	13.1
	n = 3, $[Li^+(O^{Ntf2})_2]^{-2}$	–	–	–	–	–
	n = 4, $[Li^+(O^{Ntf2})_2]^{-3}$	–	–	–	–	–
	total for 2-fold	**0**	**1.1**	**7.1**	**7.5**	**23.3**

[a]Data for k = 2–5 are shown.

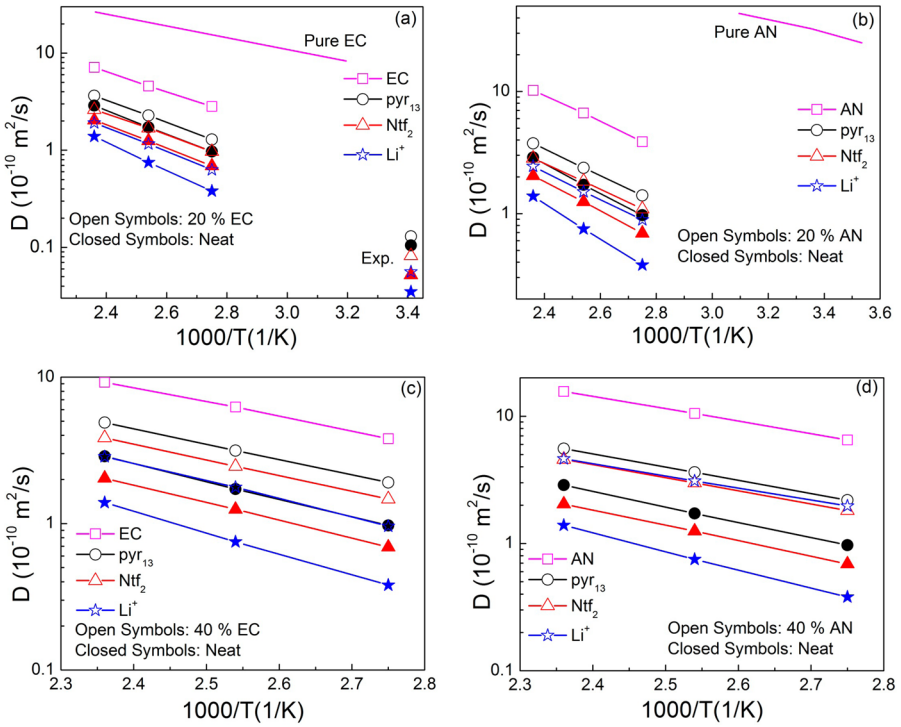

Figure 9. Self-diffusion coefficients of components in neat and diluted electrolytes as obtained from MD simulations of (a) 20% EC, (b) 20% AN, (c) 40% EC, and (d) 40% AN in ILEs. Available experimental are also shown for neat and 20% EC diluted ILEs.[6] The estimated error bars are smaller than the symbol size.

Figure 10 also shows that the enhancement of the ion mobility upon dilution has noticeable temperature dependence, the strongest one seen for the Li^+. As the temperature decreases the ratio of diffusion coefficients in the diluted and neat ILEs increases. This trend is beneficial for the lithium batteries, as the mobility of Li^+ ions would be more enhanced at room temperature and below which is the primary range for application of such batteries. This temperature dependence is likely due to plasticizing effect of the organic solvent which has a different Arrhenius dependence for mobility (smaller slope)[25,47] than the neat ILE (as shown in Figure 9, parts a and b). Therefore, when the temperature goes down the difference between pure solvent

DOI: 10.1021/jp510644k
J. Phys. Chem. B 2015, 119, 3085–3096

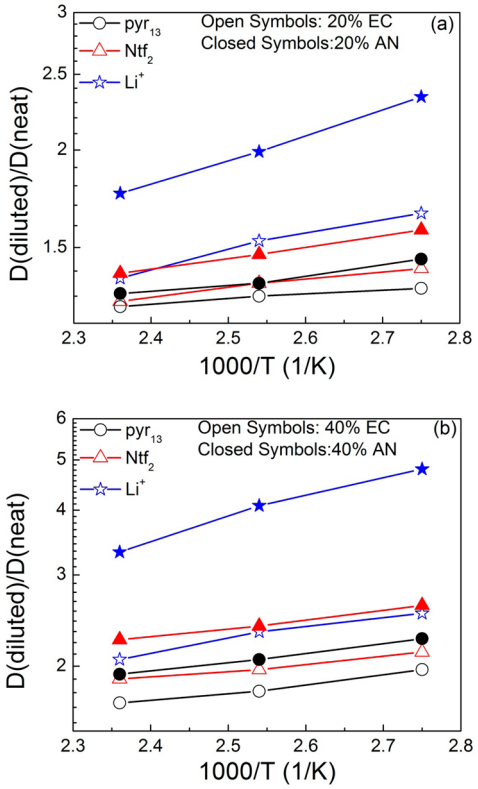

Figure 10. Ratio of self-diffusion coefficients of the components as obtained from simulations of (a) 20% and (b) 40% diluted ILEs and neat ILE as a function of temperature.

and neat ILE mobilities increases and hence the addition of solvent to ILE results in more pronounced speed up of the ions' mobility with decreasing temperature.

Ionic conductivity. The ionic conductivity from MD simulations can be calculated using the following relation

$$\lambda = \lim_{t\to\infty} \lambda^{app}(t) = \lim_{t\to\infty} \frac{e^2}{6tVK_BT} \sum_{ij}^{N} Z_i Z_j \langle [R_i(t) - R_i(0)] [R_j(t) - R_j(0)] \rangle \quad (2)$$

where $\lambda^{app}(t)$ is the apparent time-dependent conductivity, e is the electron charge, V is the volume of the simulation cell, k_B is the Boltzmann constant, T is the temperature, t is time, Z_i and Z_j are the charges of ions i and j in electrons, $R_i(t)$ is the displacement of ion i during time t, the summation is performed over all ions, $\langle\ \rangle$ denotes the ensemble average, and N is the total number of ions in the simulation cell. Determining the long-time limit of $\lambda^{app}(t)$ using eq 2 is, however, problematic even at higher temperatures due to poor statistics and higher uncertainty compared to MSD(t) and self-diffusion coefficients. Fortunately, the ionic conductivity can be decomposed into an "ideal" conductivity that would be realized if the ions motion were uncorrelated, denoted as λ_{uncorr}, and the degree to which the ion motion is uncorrelated, or α.

$$\lambda_{uncorr} = \lim_{t\to\infty} \lambda^{app}_{uncorr}(t) = \lim_{t\to\infty} \frac{e^2}{6tVK_BT} \sum_{i}^{n_i} Z_i^2 \langle [R_i(t) - R_i(0)]^2 \rangle = \frac{e^2}{VK_BT} (n_{Li}D_{Li} + n_{pyr_{13}}D_{pyr_{13}} + n_{Ntf_2}D_{Ntf_2}) \quad (3)$$

where n_i is the number of atoms of type i. The degree of uncorrelated ion motion (α) is typically measured as the ratio of the collective (total) charge transport (given by λ) to the charge transport due to self-diffusion only (the limit of uncorrelated motion), λ_{uncorr}, and is given by

$$\alpha = \frac{\lambda}{\lambda_{uncorr}} = \lim_{t\to\infty} \alpha(t) = \lim_{t\to\infty} \frac{\lambda^{app}(t)}{\lambda^{app}_{uncorr}(t)} \quad (4)$$

Thus, $\alpha = 1$ corresponds to completely uncorrelated ion motion, while $\alpha = 0$ is obtained when cations only move together with anions. Our experience indicates that reliable values of α for a given system can be extracted from the apparent $\alpha(t)$ dependence using the time range right after the transient regime.[27] For all ILEs investigated the α calculated from MD simulation lies in the range of 0.42−0.71 and are summarized in Table 5. For neat and 20% diluted electrolytes, the predicted

Table 5. Degree of Ion Dissociation (α)

T (K)	neat	20% EC	20% AN	40% EC	40% AN
423	0.71	0.61	0.60	0.53	0.47
393	0.69	0.61	0.54	0.51	0.42
363	0.67	0.59	0.56	0.50	0.42

from MD simulation α is slightly higher than the experimental value ~0.5 reported at room temperature.[6] However, the slightly lower temperature (293 K) in the measurements has likely lowered the value of α estimated experimentally. Table 5 also shows that with addition of organic solvent the degree of ion association is increasing (α is decreasing). This is consistent with previous experiments where addition of the organic solvents indeed increased the ion association in the electrolytes.[6,48,49]

The temperature dependence of ionic conductivities is shown in Figure 11. In agreement with available experimental data, addition of 20 mol % of organic solvents to ILE results in an increase of the ionic conductivity.[6,13] Despite the reduction in the number of ions per volume within the diluted ILEs, the lower viscosity of diluted electrolytes and the higher diffusion of ions contribute to the improved conductivity. Because of more

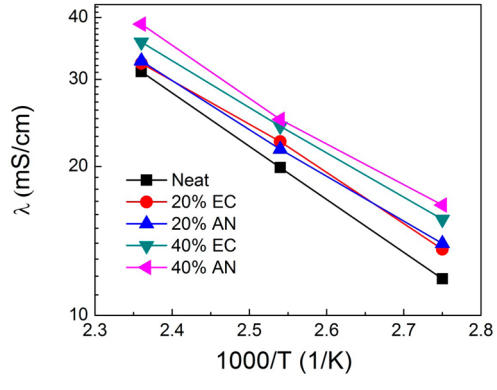

Figure 11. Ionic conductivity as a function of temperature.

DOI: 10.1021/jp510644k
J. Phys. Chem. B 2015, 119, 3085−3096

improvement of ion mobility in the electrolyte upon adding AN compared to EC we observe a slightly higher conductivity in the former. More improvement of ionic conductivity can be achieved by further addition of the solvents.

Li^+ Conductivity and Transport Mechanisms. Contribution of Li^+ to ionic conductivity (λ^{Li}) was estimated as

$$\lambda^{Li} = \frac{n_{Li}D_{Li}}{n_{Li}D_{Li} + n_{pyr_{13}}D_{pyr13} + n_{Ntf2}D_{Ntf2}}\lambda \quad (5)$$

and is shown in Figure 12. Li^+ conductivity, as expected, has improved upon addition of organic solvent, in particular with

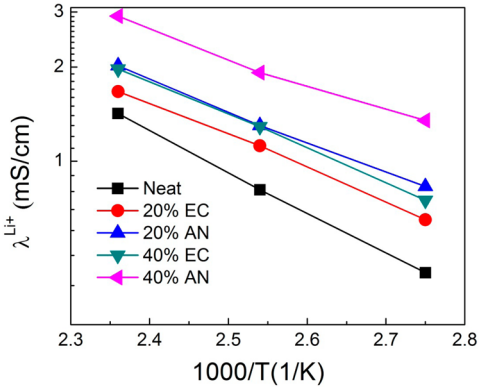

Figure 12. Li conductivity as a function of temperature.

addition of AN molecules. At higher temperatures (423 K) addition of 20% AN has resulted in increase of Li^+ conductivity by almost 40% and doubled when AN concentration in ILE increased to 40%. At lower temperatures (363 K) the Li^+ conductivity has increased by a factor of 4 with addition of AN solvent.

Because of importance of the Li^+ transport on the efficacy of ILEs in lithium battery applications, we have examined the influence of organic solvents on the mechanisms of Li^+ cation transport in ILEs. It is generally recognized that the Li^+ transport has contributions from the motion with its coordination shell (vehicular mechanism) and from exchanging Ntf_2 anions in the first coordination shell (structure diffusion mechanism). In order to understand the relative importance of these mechanisms we have analyzed the Li^+–N^{Ntf2} residence times as a function of temperature and solvent concentration. The residence time autocorrelation function (ACF) for the N^{Ntf2} anions in the first coordination shell of Li^+ was calculated using

$$p_{Li^+-N^{Ntf2}} = \frac{\langle H_{ij}(t)H_{ij}(0)\rangle}{\langle H_{ij}(0)H_{ij}(0)\rangle} \quad (6)$$

where $H_{ij}(t) = 1$ when $r(Li^+–N^{Ntf2}) < 5.3$ Å, respectively, and zero otherwise. The ensemble average denoted by $\langle\ \rangle$ was taken over all Li^+ cations in the system using multiple time origins. This ACF decays from unity to zero when all Li^+ cations have completely exchanged the Ntf_2 anions in their solvation shells. It was found that these ACFs can be well fit with the Kohlrausch–Williams–Watts (KWW) stretched exponential function.[50]

$$p_{Li^+-N^{Ntf2}} = A\ \exp[-(t/\tau_{KWW})^{\beta}] \quad (7)$$

The ACFs and their fits with KWW functions are shown in Figure SI.4. The decay of the ACFs to zero occurs on a time scale of several ns, indicating that the correlations (binding) between any given Li^+–Ntf_2 pair are not long-lived. Given the result that exponent β obtained from the fits is around 0.9, we believe the Li–Ntf_2 ACFs decay has almost a single relaxation time behavior. When organic solvents were added to neat ILE a faster decay of ACF was obtained indicating the reduction in Li^+–Ntf_2 correlations (i.e., a relatively fast Ntf_2 exchange). AN again showed a more influence on the Li^+–N^{Ntf2} ACF compared to EC solvent. The characteristic lifetime (τ) of the solvation shell, i.e., the time needed for the Li^+ cation to completely change the solvating anions, was calculated by integrating the ACF as

$$\tau = \int_0^{\infty} A\ \exp[-(t/\tau_{KWW})^{\beta}]\ dt \quad (8)$$

and are shown in Figure 13 as a function of temperature. As expected, addition of organic solvents in the ILEs encouragingly

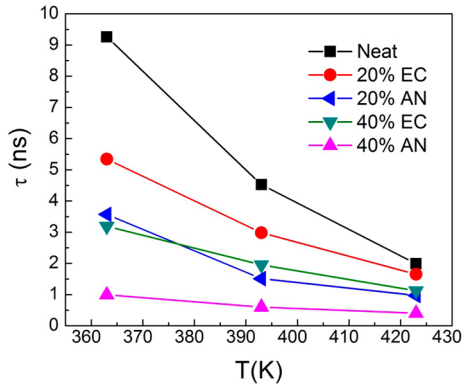

Figure 13. Characteristic residence times (τ) of Ntf_2 in the first coordination shell of Li^+ as a function of temperature.

reduces the lifetime (τ) of Li^+ solvation shell, therefore enhancing the structure diffusion mechanism. Note that the decrease of τ with addition of solvent has a noticeable temperature dependence, providing significantly more reduction of the lifetime at lower temperatures. This trend is consistent with the observed temperature dependence of the ion self-diffusion coefficient speed up factors shown in Figure 10. In fact the product of τ and D_{Li+} gives almost a constant value as a function of temperature. This indicates a strong correlation/coupling between Li^+ coordination shell lifetime and Li^+ mobility. If the added organic solvent acted only as a plasticizer, i.e., improving the mobility of $Li^+(Ntf_2)_n]^{(n-1)-}$ complexes but not affecting the complexes' lifetime, then the τ^*D_{Li+} would show a strong temperature dependence. An absence of such dependence in our data indicates that the observed improvement of Li^+ mobility with addition of the solvent is directly related to ability of solvent molecules to reduce the lifetime of $Li^+(Ntf_2)_n]^{(n-1)-}$ complexes.

CONCLUSIONS

Atomistic MD simulations using polarizable force fields showed that addition of two organic solvents (AN or EC) to ionic liquid based electrolyte (ILE) containing Li salt is able to noticeably improve the ion transport properties in the ILEs. Added AN and EC solvents competed for the Li^+ cation coordination by replacing Ntf_2 anions, changing the Li^+–Ntf_2 binding pattern and residence times, and enhancing ion diffusion coefficients. AN have shown slightly higher affinity to Li^+ compared to EC, displacing more Ntf_2 anions from the Li^+ coordination shell and more significantly enhancing Li^+ transport. Moreover, affected

DOI: 10.1021/jp510644k
J. Phys. Chem. B 2015, 119, 3085–3096

the Li^+ coordination structure by changing the bidentate anions to monodentate as well as replacing anions in the first coordination shells of Li^+ cations. Incorporation of organic solvent in the electrolyte also reduces the Li^+-N^{Ntf2} correlations resulting in enhancing the structure diffusion mechanism of Li^+ transport which in turn leads to improved Li^+ self-diffusion coefficient and conductivity due to Li^+, especially at lower temperatures which is the most critical for a battery operation.

■ ASSOCIATED CONTENT

Supporting Information

Representative snapshots of Li ion first coordination shell and additional data on radial distribution functions and anions residence autocorrelation functions obtained from MD simulations. This material is available free of charge via the Internet at http://pubs.acs.org.

■ AUTHOR INFORMATION

Corresponding Author

*(D.B.) E-mail: d.bedrov@utah.edu.

Notes

The authors declare no competing financial interest

■ ACKNOWLEDGMENTS

The authors are grateful for financial support of this work by the U.S. Department of Energy through Grant DE-AC02-05CH11231 on PO No. 6838611 to University of Utah and by the Army Research Laboratory under Cooperative Agreement Number W911NF-12-2-0023. The views and conclusions contained in this document are those of the authors and should not be interpreted as representing the official policies, either expressed or implied, of the Army Research Laboratory or the U.S. Government.

■ REFERENCES

(1) Diaw, M.; Chagnes, A.; Carre, B.; Willmann, P.; Lemordant, D. Mixed Ionic Liquid as Electrolyte for Lithium Batteries. *J. Power Sources* **2005**, *146*, 682−684.

(2) Best, A. S.; Bhatt, A. I.; Hollenkamp, A. F. Ionic Liquids With The Bis(fluorosulfony)imide Anion: Electrochemical Properties and Applications in Battery Technology. *J. Electrochem. Soc.* **2010**, *157* (8), A903−A911.

(3) Guerfi, A.; Dontigny, M.; Charest, P.; Petitclerc, M.; Lagace, M.; Vijh, A.; Zaghib, K. Improved Electrolytes for Li-ion Batteries: Mixtures of Ionic Liquid and Organic Electrolyte with Enhanced Safety and Electrochemical Performance. *J. Power Sources* **2010**, *195*, 845−852.

(4) Sun, X. G.; Dai, S. Electrochemical investigations of Ionic Liquids with Vinylene carbonate for Applications in Rechargeable Lithium Ion Batteries. *Electrochim. Acta* **2010**, *55*, 4618−4626.

(5) Ohno, H. H. Functional Design of Ionic Liquids. *Bull. Chem. Soc. Jpn.* **2006**, *79*, 1665−1680.

(6) Bayley, P. M.; Lane, G. H.; Rocher, N. M.; Clare, B. R.; Best, A. S.; MacFarlane, D. R.; Forsyth, M. Transport Properties of Ionic Liquid Electrolytes with Organic Diluents. *Phys. Chem. Chem. Phys.* **2009**, *11*, 7202−7208.

(7) Seki, S.; Kobayashi, Y.; Miyashiro, H.; Ohno, Y.; Usami, A.; Mita, Y.; Kihira, N.; Watanabe, M.; Terada, N. Lithium Secodary Batteries Using Modified-Imidazolium Room-Temperature Ionic Liquids. *J. Phys. Chem. Phys.* **2006**, *110*, 10228−10230.

(8) Choi, J. A.; Eo, S. M.; MacFarlane, D. R.; Forsyth, M.; Cha, E.; Kim, D. W. Effect of Organic Additives on The Cycling Performances of Lithium Metal Polymer Cells. *J. Power Sources* **2008**, *178*, 832−836.

(9) Sato, T.; Maruo, T.; Marukane, S.; Takagi, K. Ionic Liquids Containing Carbonate Solvent as Electrolytes for Lithium Ion Cells. *J. Power Sources* **2004**, *138*, 253−261.

(10) Holzapfel, M.; Jost, C.; Novak, P. Stable Cycling of Graphite in An Ionic Liquid Based Electrolyte. *Chem. Commun.* **2004**, *10*, 2098−2099.

(11) Katayama, Y.; Yukumoto, M.; Miura, T. Electrochemical Intercalation of Lithium into Graphite in Room-Temperature Molten Salt Containing Ethylene Carbonate. *Electrochem. Solid-State Lett.* **2003**, *5*, A96−A97.

(12) Bayley, P. M.; Best, A. S.; MacFarlane, D. R.; Forsyth, M. The Effect of Coordinating and Non-coordinating Additives on The Transport Properties in Ionic Liquid Electrolytes for Lithium Batteries. *Phys. Chem. Chem. Phys.* **2011**, *13*, 4632−4640.

(13) Bayley, P. M.; Lane, G. H.; Lyons, L. J.; MacFarlane, D. R.; Forsyth, M. Undoing Lithium Ion Association in Ionic Liquids Through The Complexation by Oligoethers. *J. Phys. Chem. C* **2010**, *114*, 20569−20576.

(14) Hardwick, L. J.; Holzapfel, M.; Wokaun, A.; Novak, P. Raman Study of Lithium Coordination in EMI-TFSI Additives Systems as Lithium Ion Battery Ionic Liquid Electrolytes. *J. Raman Spectrosc.* **2007**, *38*, 110−112.

(15) Lassègues, J.; Grondin, J.; Talaga, D. Lithium Solvation in Bis(trifluoromethanesulfonyl) imide-based Ionic Liquids. *Phys. Chem. Chem. Phys.* **2006**, *8*, 5629−5632.

(16) Lassegues, J. C.; Grondin, J.; Aupetit, C.; Johansson, P. Spectroscopic Identification of the Lithium Ion Transporting Species in LiTFSI-Doped Ionic Liquids. *J. Phys. Chem. A* **2009**, *113*, 305−314.

(17) Pitawala, J.; Martinelli, A.; Johansson, P.; Jacobsson, P.; Matic, A. Coordination and Interactions in a Li-Salt Doped Ionic Liquid. *J. Non-Cryst. Solids* **2015**, *407*, 318−323.

(18) Seo, D. M.; Borodin, O.; Han, S. D.; Boyle, P. D.; Henderson, W. A. Electrolyte Solvation and Ionic Association II. Acetonitrile-Lithium Salt Mixtures: Highly Dissociated Salts. *J. Electrochem. Soc.* **2012**, *159*, A1489−A1500.

(19) Umebayashi, Y.; Yamaguchi, T.; Fukuda, S.; Mitsugi, T.; Takeuchi, M.; Fujii, K.; Ishiguro, S. Raman Spectroscopic Study on Alkaline Metal Ions Solvation in 1-Butyl-3-methylimidazolium Bis-(trifluoromethanesulfonyl) Amide Ionic Liquid. *Anal. Sci. Jpn.* **2008**, *24*, 1297−1304.

(20) Shirai, A.; Fujii, K.; Seki, S.; Umebayashi, Y.; Ishiguro, S.; Ikeda, Y. A study on Solvation of Lithium Ion in N,N-diethyl-N-methyl-N-(2-methoxy-ethyl)ammonium Bis(trifluoromenthanesulfonyl)imide Using Raman and Multinuclear NMR Spectroscopy. *Anal. Sci. Jpn.* **2008**, *24*, 1291−1296.

(21) Borodin, O.; Smith, G. D.; Henderson, W. The Li^+ Cation Environment and Transport Mechanisms in Propylpyrrolidinium$^+$/$TFSI^-$ Ionic Liquid. *J. Phys. Chem. B* **2006**, *110*, 16879−16886.

(22) Umebayashi, Y.; Hamano, H.; Seki, S.; Minofar, B.; Fujii, K.; Hayamizu, K.; Tsuzuki, S.; Kameda, Y.; Kohara, S.; Watanabe, M. Liquid Structure of and Li^+ Ion Solvation in Bis(trifluoromethanesulfonyl)-amide Based Ionic Liquids Composed of 1-ethyl-3-methylimidazolium and N-methyl-N-propylpyrrolidinium Cations. *J. Phys. Chem. B* **2011**, *115*, 12179−12191.

(23) Monteiro, M. J.; Bazito, F. F. C.; Aiqueira, L. J. A.; Ribiro, M. C. C.; Torresi, R. M. Transport Coefficients, Raman Spectroscopy, and Computer Simulation of Lithium Salt Solutions in an Ionic Liquid. *J. Phys, Chem. B* **2008**, *112*, 2102−2109.

(24) Borodin, O.; Smith, G. D. Structure and Dynamics of N-Methyl-N-propylpyrrolidinium Bis(trifluoromethanesulfonyl)imide Ionic Liquid from Molecular Dynamics Simulations. *J. Phys. Chem. B* **2006**, *110*, 11481−11490.

(25) Bauschlicher, C. W.; Haskins, J. B.; Bucholz, E. W.; Lawson, J. W.; Borodin, O. Structure and Energetics of Li^+-$(BF_4^-)_n$, and Li^+-$(TFSI^-)_n$: Ab Initio And Polarizable Force Field Approaches. *J. Phys. Chem. B* **2014**, *118*, 10785−10794.

(26) Borodin, O.; Smith, G. D. Development of The Many-Body Polarizable Force Fields For Lithium-Battery Applications: 1. Ether, Alkane And Carbonate-Based Solvents. *J. Phys. Chem. B* **2006**, *110*, 6279−6292.

(27) Borodin, O. Polarizable Force Field Development and Molecular Dynamics Simulations of Ionic Liquids. *J. Phys. Chem. B* **2009**, *113*, 11463−11478.

DOI: 10.1021/jp510644k
J. Phys. Chem. B 2015, 119, 3085−3096

(28) Borodin, O.; Henderson, W. A.; Fox, E. T.; Berman, M.; Gobet, M.; Greenbaum, S. Influence of Solvent on Ion Aggregation and Transport in PY_{15}TFSI Ionic Liquid-Aprotic Solvent Mixtures. *J. Phys. Chem. B* **2013**, *117*, 10581−10588.
(29) Lesch, V.; Jeremias, S.; Moretti, A.; Passerini, S.; Heuer, A.; Borodin, O. A Combined Theoretical and Experimental Study of the Influence of Different Anion Ratios on Lithium Ion Dynamics in Ionic Liquids. *J. Phys. Chem. B* **2014**, *118*, 7367−7375.
(30) Jow, T. R.; Xu, K.; Borodin, O.; Ue, M.*Electrolytes for Lithium and Lithium-Ion Batteries*; Springer: New York, 2014.
(31) Solano, C. J. F.; Jeremias, S.; Paillard, E.; Beljonne, D.; Lazzaroni, R. A Joint Theoretical/Experimental Study of the Structure, Dynamics, and Li^+ Transport in Bis([tri]fluoro[methane]sulfonylimide [T]FSI-based Ionic Liquids. *J. Chem. Phys.* **2013**, *139*, 034502.
(32) Li, Z.; Smith, G. D.; Bedrov, D. Li^+ Solvation and Transport Properties in Ionic Liquid/Lithium Salt Mixtures: A Molecular Dynamics Simulation Study. *J. Phys. Chem. B* **2012**, *116*, 12801−12809.
(33) McOwen, D. W.; Seo, D. M.; Borodin, O.; Vatamanu, J.; Boyle, P. D.; Henderson, W. A. Concentrated Electrolytes: Decrypting Electrolyte Properties and Reassessing AI Corrosion Mechanisms. *Energy Environ. Sci.* **2014**, *7*, 416−426.
(34) Arulepp, M.; Permann, L.; Leis, J.; Perkson, A.; Rumma, K.; Janes, A.; Lust, E. Influence of The Solvent Properties on The Characteristics of A Double Layer Capacitor. *J. Power Sources* **2004**, *133*, 320−328.
(35) Desphande, A.; Kariyawasam, L.; Dutta, P.; Banerjee, S. Enhancement of Lithium Ion Mobility in Ionic Liquid Electrolytes in Presence of Additives. *J. Phys. Chem. C* **2013**, *117*, 25343−25351.
(36) Martyna, G. J.; Tobias, D. J.; Klein, M. L. Constant Pressure Molecular Dynamics Algorithms. *J. Chem. Phys.* **1994**, *101*, 4177−4189.
(37) Martyna, G. J.; Tucherman, M. E.; Tobias, D. J.; Klein, M. L. Explicit Reversible Integrators for Extended Systems Dynamics. *Mol. Phys.* **1996**, *87*, 1117−1157.
(38) Palmer, B. J. Direct Application of Shake to the Velocity Verlet Algorithm. *J. Comput. Phys.* **1993**, *104*, 470−472.
(39) Matsunoto, K.; Hagiwara, R.; Tamada, O. Coordination Environment Around The Lithium Cation in Solid Li_2(EMIm)(N-$(SO_2CF_3)_2)_3$ (EMIm = 1-Ethyl-3-Methylimidazolium): Structural Clue of Ionic Liquid Electrolytes for Lithium Batteries. *Solid State Sci.* **2006**, *8*, 1103−1107.
(40) Saito, Y.; Umecky, T.; Niwa, J.; Sakai, T.; Maeda, S. Existing Condition and Migration Property of Ions in Lithium Electrolytes with Ionic Liquid Solvent. *J. Phys. Chem. B* **2007**, *111*, 11794−11802.
(41) Umecky, T.; Saito, Y.; Okumura, Y.; Maeda, S.; Sakai, T. Ionization Condition of Lithium Ionic Liquid Electrolytes under the Solvation Effect of Liquid and Solid Solvents. *J. Phys. Chem. B* **2008**, *112*, 3357−3364.
(42) Castriota, M.; Caruso, T.; Agostino, R. G.; Cazzanelli, E.; Henderson, W. A.; Passerini, S. Raman Investigation of the Ionic Liquid N-Methyl-N-propylpyrrolidinium Bis(trifluoromethanesulfonyl)imide and Its Mixture with $LiN(SO_2CF_3)_2$. *J. Phys. Chem. A* **2005**, *109*, 92−96.
(43) Haskins, J. B.; Bennett, W. R.; Wu, J. J.; Hernandez, D. M.; Borodin, O.; Monk, J. D.; Bauschlicher, C. W., Jr.; Lawson, J. W. Computational and Experimental Investigation of Li-doped Ionic Liquid Electrolytes:[pyr14][TFSI], [pyr13][FSI], and [EMIM][BF_4]. *J. Phys. Chem. B* **2014**, *118*, 11295−11309.
(44) Fox, E. T.; Paillard, E.; Borodin, O.; Henderson, W. A. Physicochemical Properties of Binary Ionic Liquid-Aprotic Solvent Electrolyte Mixtures. *J. Phys. Chem. C* **2013**, *117*, 78−84.
(45) Borodin, O.; Smith, G. D. LiTFSI Structure and Transport in Ethylene Carbonate from Molecular Dynamics Simulations. *J. Phys. Chem. B* **2006**, *110*, 4971−4947.
(46) Umebayashi, Y.; Mori, S.; Fujii, K.; Tsuzuki, S.; Seki, S.; Hayamizu, K.; Ishiguro, S. Raman Spectroscopic Studies and Ab Initio Calculations on Conformational Isomerism of 1-Butyl-3-methylimidazolium Bis-(trifluoromethanesulfonyl)amide Solvated to a Lithium Ion in Ionic Liquids: Effects of the Second Solvation Sphere of the Lithium Ion. *J. Phys. Chem. B* **2010**, *114*, 6513−6521.
(47) Chaban, V. V.; Voroshylova, L. V.; Kalugin, O. N.; Prezhdo, O. V. Acetonitrile Boosts Conductivity of Imidazolium Ionic Liquids. *J. Phys. Chem. B* **2012**, *116*, 7719−7727.
(48) Li, W.; Zhang, Z.; Han, B.; Hu, S.; Xie, Y.; Yang, G. Effect of Water and Organic Solvents on The Ionic Dissociation of Ionic Liquids. *J. Phys. Chem. B* **2007**, *111*, 6452−6456.
(49) Tokuda, H.; Baek, S. J.; Watanabe, M. Room Temperature Ionic Liquid-Organic Solvent Mixtures: Conductivity and Ionic Association. *Electrochemistry* **2005**, *73*, 620−622.
(50) Williams, G.; Watts, D. C. Non-symmetrical Dielectric Relaxation Behaviour Arising from A Simple Empirical Decay Function. *Trans. Faraday Soc.* **1970**, *66*, 80−85.
(51) Schindler, W.; Zerda, T. W.; Jonas, J. High Pressure Raman Study of Intermolecular Interactions and Fermi Resonance in Liquid Ethylene Carbonate. *J. Chem. Phys.* **1984**, *81*, 4306−4313.
(52) Nikam, P. S.; Shirsat, L. N.; Hasan, M. Densities and Viscosity Studies for Binary Mixtures of Acetonitrile with Methanol, Ethanol, Propan-1-ol, Propan-2-ol, Butan-2-ol, 2-methylproan-1-ol, and 2-methylpropan-2-ol at (298.15, 33.15, 308.15, and 313.15) K. *J. Chem. Eng. Data* **1998**, *43*, 732−737.

DOI: 10.1021/jp510644k
J. Phys. Chem. B 2015, 119, 3085−3096